

Growth of electrodeposited γ -manganese dioxide from a suspension bath

E. PREISLER

Hoechst AG, Werk Knapsack, D-5030 Hürth/Germany

Received 23 October 1988; revised 16 February 1989

The addition of solid particles of manganese oxides to the electrolyte of a manganese dioxide production bath (suspension bath process = SBP) allows the anodic current density to be increased to values more than twice that used in the conventional EMD process. This is possible even with the use of titanium anodes which are sensitive to passivation if the current density exceeds critical values. Analysis of deposition conditions and properties of the SBP-EMD shows that the SBP-EMD resembles an EMD which has been deposited at very low current densities. These low current densities are realized by the adsorption of the suspended particles on the anode surface, thereby promoting dendritic crystal growth on the adsorbed particles and increasing the real anode surface by up to a factor of ten. This assumption is able to explain most of the properties found for the SBP-EMD, e.g. X-ray pattern, potential drop, hardness of the deposit, low specific surface area, low content of combined water and high electronic conductivity.

1. Introduction

Usually, electrodeposited manganese dioxide (EMD) is produced on a technical scale by anodic oxidation of manganese ions at temperatures of 90–95°C in electrolytes containing sulphuric acid. For a long time the most widely used anode material was graphite; but nowadays titanium is increasingly being used because of its good corrosion resistance which enables a service life of several years to be achieved.

One of the problems encountered with titanium anodes is the restriction of anodic current density to relatively low values of 0.8 to 1.1 A dm⁻² [1, 2]. Furthermore, the quality of EMD is reduced when higher current densities are used [3].

In contrast, remarkably high current densities, up to 2 A dm⁻², can be applied in the so-called suspension bath process (SBP), as developed by Misawara *et al.* for Japan Metals and Chemicals Co., Ltd [4, 5]. The use of such high current densities conflicts with explanations given earlier for the behaviour of titanium covered with manganese dioxide [3]. Furthermore, SBP-EMD exhibits X-ray diffraction patterns very near to γ -MnO₂, while conventional EMD under similar deposition conditions shows clear ϵ -MnO₂ patterns [12]. This is also conflicting with what is known on the deposition mechanism and structure of EMD [6].

There is little published information on the growth of EMD in a suspension bath. The special feature of the SBP is the addition of fine particles of manganese oxide to the electrolyte. These particles can be manganese dioxide or oxides of lower manganese valency, such as Mn₂O₃ or Mn₃O₄. The oxides have to be milled to a low grain size to ensure a homogeneous suspension in the electrolyte. Yoshio and Noguchi [7]

observed that the anode potential was lowered by 100 mV on addition of 0.1 g/l of particles to the bath. No significant difference could be found from the addition of γ -MnO₂, β -MnO₂ or α -Mn₂O₃ proving that the chemical state of these manganese oxide particles plays only a minor role. It may be of importance that even nonmanganese particles can produce a similar, though less efficient, effect on the EMD anodes [8].

Yoshio and Noguchi [7] give some results for the dependence of X-ray diffraction patterns, and of electrode potential, on the particle concentration and on gas additions to the electrolyte. For the case of gas additions they suggested that SBP-EMD appears similar to EMD obtained from a sulphate bath at low current density.

The purpose of this paper is to show that, by adsorption of manganese-containing particles, the effective anode surface is increased remarkably up to a factor of 10 or more and, therefore, that the effective current density is correspondingly reduced. This is quite independent of the presence of nitrogen gas. This assumption enables the properties of SBP-EMD and the behaviour of the titanium anode in the suspension bath to be explained by the same model which has been used for the deposition of EMD from sulphate electrolyte and for fibrous EMD from nitrate or chloride baths [6].

2. Experimental

2.1. Electrolysis

The experimental conditions used for the preparation of SBP-EMD were very similar to those for a conventional process and are listed in Table 1. Anodes of

Table 1. Conditions of MnO_2 electrodeposition

	conventional bath	suspended particles bath
Electrolyte		
$c_{H_2SO_4}/M$	0.4–0.7	0.4–0.7
c_{MnSO_4}/M	0.3–0.5	0.3–0.5
$c_{susp. particles}/g\ l^{-1}$	–	0.01–2
temperature/ $^{\circ}C$	90–95	90–95
cathodes	graphite	graphite
anodes	titanium (sheet or sintered plate)	titanium (sheet or sintered plate)
current density/ $A\ dm^{-2}$	0.05–1.0	0.85–2.5
deposition time depends on thickness of deposit intended.		

rolled titanium sheet, 2 mm thick, or sintered titanium plates, 8 mm thick, both with a length of 60 cm and a width of 8 cm were used. The electrolyte was pumped through the cell via a bypass including a heat exchanger. Pre-selected volumes of a concentrated suspension of particles in neutral electrolyte were added at defined time intervals in order to maintain a fairly constant particle concentration in the cell electrolyte. Manganese ion and sulphuric acid concentrations were kept constant by the usual method of substituting continuously a part of the cell electrolyte by neutral manganese sulphate solution.

2.2. Suspensions of manganese oxides

Manganese oxides were milled to a mean particle diameter less than 20 μm and suspended in a neutral manganese sulphate solution. The suspensions were stored in a stirred condition.

2.3. Suspensions of manganese oxide hydrates

According to a new SBP [10] suspensions of hydrated manganese oxides were produced by oxidizing a

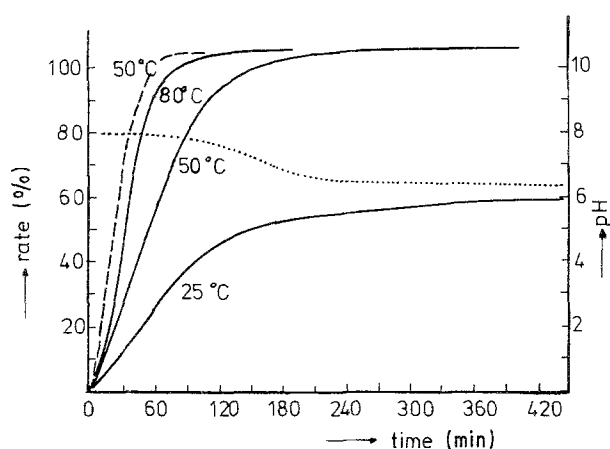


Fig. 1. Oxidation of manganese hydroxide by air (solid lines) or oxygen (broken line) at different temperatures. Dashed line indicates the corresponding change of pH value for the 50 $^{\circ}C$ reaction.

manganese sulphate solution with potassium permanganate or (when potassium ions were not desired in the electrolyte) by adding sodium hydroxide to a bypass stream of the recovered neutral electrolyte and oxidizing the resulting precipitate of manganese hydroxide by air (Fig. 1). Both reactions were performed at about 50–60 $^{\circ}C$.

2.4. Determination of the concentration of suspended particles

Since all the manganese compounds used for suspensions contained manganese of a valency higher than 2, it was convenient to determine the quantity of manganese 4 introduced by the suspended particles into the electrolyte. This was done by adding to the sample volume an excess of arsenous acid and heating the solution until all particles had dissolved. The excess arsenous acid was titrated with standardized ceric sulphate solution using ferroin as indicator and some osmium tetroxide as catalyst. The particle concentration is expressed as milligrams or grams of manganese dioxide per litre.

Conventional methods were used for other determinations.

3. Results

3.1. Macrostructure

The most obvious difference between conventional EMD and SBP-EMD deposits is the appearance of the surface. EMD has a smooth surface covered with a network of fine cracks which emerge when the deposits cool after removal from the hot bath. Sometimes, especially at higher current densities or at non-steady-state deposition conditions, some larger cracks and even descaling of the deposit are observed. The surface of SBP-EMD is very rough, no fine cracks can be seen and descaling only happens occasionally at low concentrations of suspended particles and exceptionally high current densities (Fig. 2). Sintered titanium anodes [11] showed less descaling than rolled titanium sheet anodes.

The roughness of the surface is the result of two effect consisting of: a macroscopic system of elevations which reflects the influence of the electrolyte flow on the deposit and a much finer structure of cauliflower-like appearance (Fig. 3). The latter is a typical consequence of the presence of particles in the electrolyte, while the former clearly shows that the adsorption of particles also depends on the hydrodynamic state of the electrolyte at the anode surface.

Cross sections through deposits of EMD and SBP-EMD parallel to the direction of growth are presented in Fig. 4. The adsorption of suspended particles happens from the beginning of their addition. A cross section through SBP-EMD parallel to its surface shows large areas of macropores. These are of very irregular shape and extend to several hundreds of micrometers (Fig. 5).

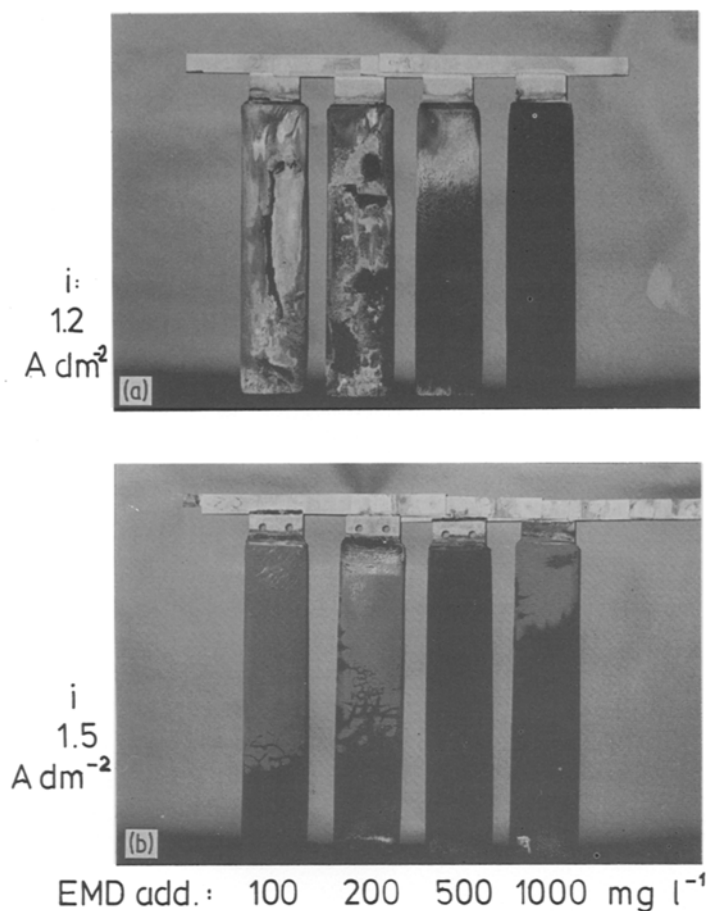


Fig. 2. Titanium anodes from suspension bath electrolysis with different concentrations of suspended EMD particles. (a) sandblasted titanium sheet anode (2 mm thick); (b) sintered titanium anode (8 mm thick); H_2SO_4 concentration; $0.45\text{--}0.5 \text{ mole l}^{-1}$; $T = 95^\circ\text{C}$.

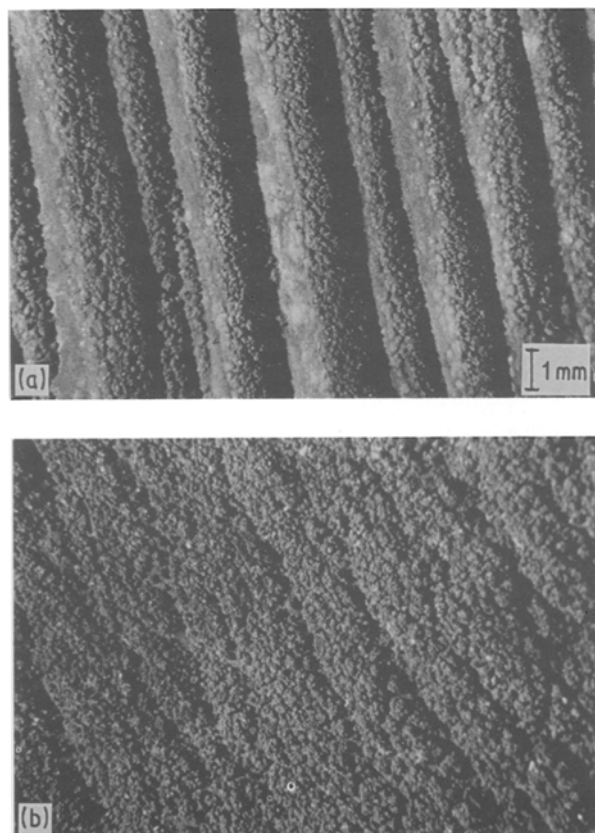


Fig. 3. Surface of a suspension bath EMD electrode. (a) area of strong influence of the electrolyte flow; (b) area of small influence.

A more detailed picture of the appearance of the surface is given by the scanning electron microscope (Fig. 6a,b). It is interesting that this surface structure was obtained regardless of the type of manganese-containing particles e.g. EMD, $\beta\text{-MnO}_2$, $\alpha\text{-Mn}_2\text{O}_3$ or $\text{MnO}_{1.7} \cdot x\text{H}_2\text{O}$ which resulted from disproportionation of hydrated hausmannite particles by the sulphuric acid of the hot cell electrolyte (Fig. 7). Differences between the compounds exist with regard to the concentrations of the particles that were necessary to produce such typical surfaces. The hydrated $\text{MnO}_{1.7}$ proved to be the most effective one; much less effective is $\beta\text{-MnO}_2$. There are also some differences in respect of the type of dendritic growth. Contrary to the findings of Yoshio and Noguchi [7] it was not necessary to introduce a stream of nitrogen.

3.2. Mesostructure

From the above it is clear that SBP-EMD deposits are highly porous. While EMD contains only meso- or micropores with diameters no more than some hundreds of nanometers the pores in SBP-EMD must be regarded mainly as macropores or even holes. Therefore, the block density of SBP-EMD varies considerably and matches in some cases the low block density of conventional EMD which is often found to be 4.00 g cm^{-3} .

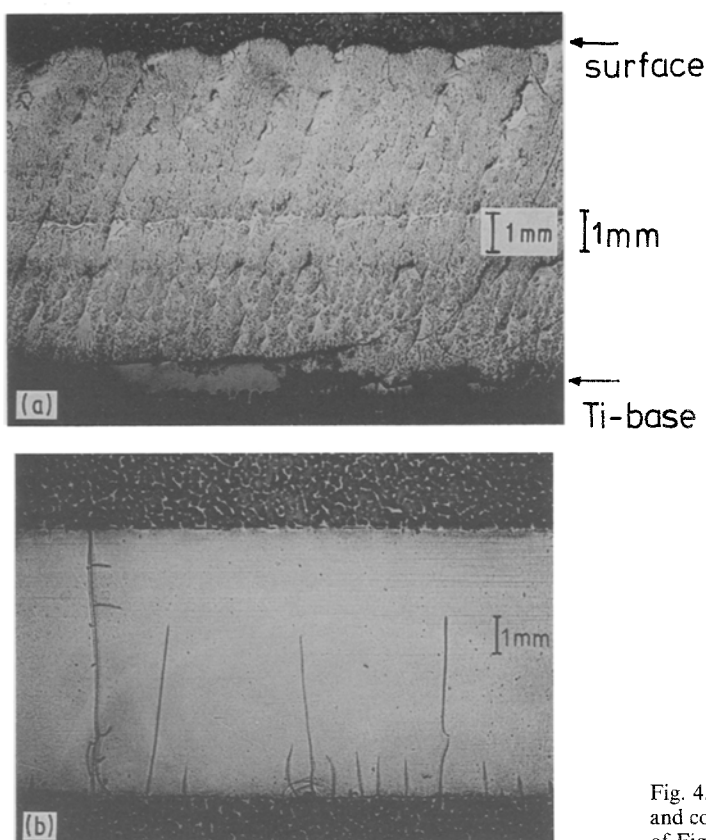


Fig. 4. Cross sections through a suspension bath EMD deposit (a) and conventional EMD (b). Section (a) corresponds to the area (a) of Fig. 3.

It is informative to compare the active surface of SBP-EMD with that of conventional EMD (Fig. 8). The value of the BET-surface of the SBP-EMD deposited at a current density of 2.5 A dm^{-2} corresponds to that of an EMD deposited at a current density of only 0.5 A dm^{-2} . Other corresponding values are 1 A dm^{-2} (SBP-EMD) and 0.08 A cm^{-2} (EMD). If the sulphate anion exerts the same influence on SBP-EMD as on EMD it is possible to conclude that SBP-EMD is deposited at real current densities which are significantly lower than the formal current densities.

The relation between active surface and concentration of bound water [6] reveals that at the same BET-area significantly less water is incorporated into the deposited SBP-EMD than in FEMD, which is

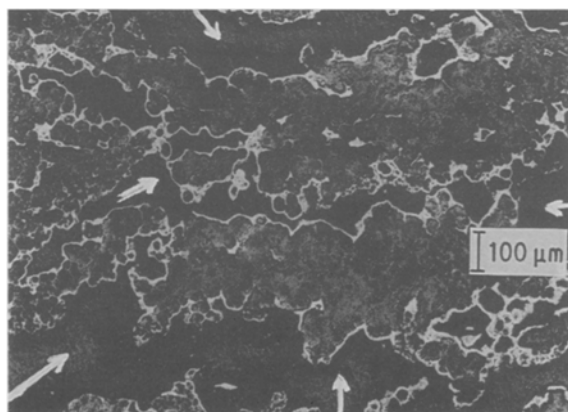


Fig. 5. Cross section through suspension bath EMD parallel to the surface. The arrows indicate the areas filled with the embedding resin.

again an indication of a low real current density for SBP-EMD (Fig. 9). This may be explained by a greater number of cation vacancies in ϵ - MnO_2 than in SBP-EMD (γ - MnO_2) [15].

3.2.1. Microstructure. It has been shown [6] that the structure of an electrodeposited manganese dioxide depends largely on the current density of deposition: high current densities produce ϵ - MnO_2 [12] while low current densities cause the growth of γ - MnO_2 [13]. A corresponding change of the X-ray diffraction patterns is tentatively measured by the ratio, Q_i , of the peak heights of the most characteristic peaks of γ - and ϵ - MnO_2 : θ ($\text{CuK}\alpha$) = 11.0° C and θ ($\text{CuK}\alpha$) = 18.5 (Fig. 10). At a current density of 0.03 A cm^{-2} a rather pronounced γ - MnO_2 pattern is obtained having $Q_i \sim 1.5$ while a typical ϵ - MnO_2 gives $Q_i \sim 0.35$.

It is perhaps not surprising that particle type, size, and concentration, and current density have a great influence on the appearance of the SBP-EMD deposit:

the formation of γ - MnO_2 is enhanced by

- a higher number of particles per unit volume
- smaller particle size
- γ - MnO_2 or ϵ - MnO_2 particles
- a lower current density

the γ - MnO_2 formation is retarded by

- lower temperature
- coarse particles
- β - MnO_2 particles
- a higher current density

This is shown in Figs 11 and 12.

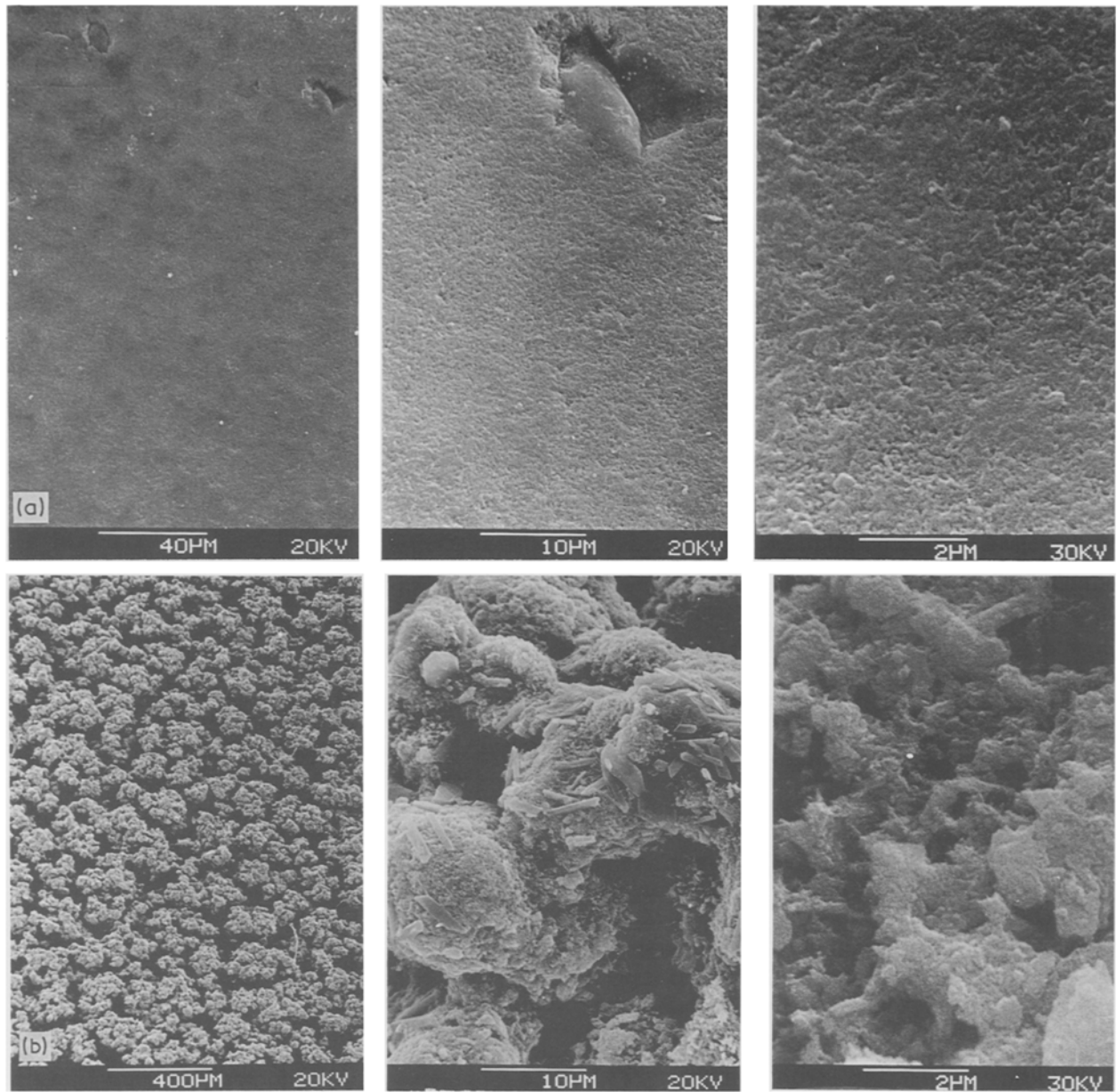


Fig. 6. Surfaces of conventional EMD (a) and suspension bath EMD (b) by scanning electron microscopy (notice that the corresponding pictures of the left row differ in magnification). Suspended particles: EMD $< 20 \mu\text{m}$.

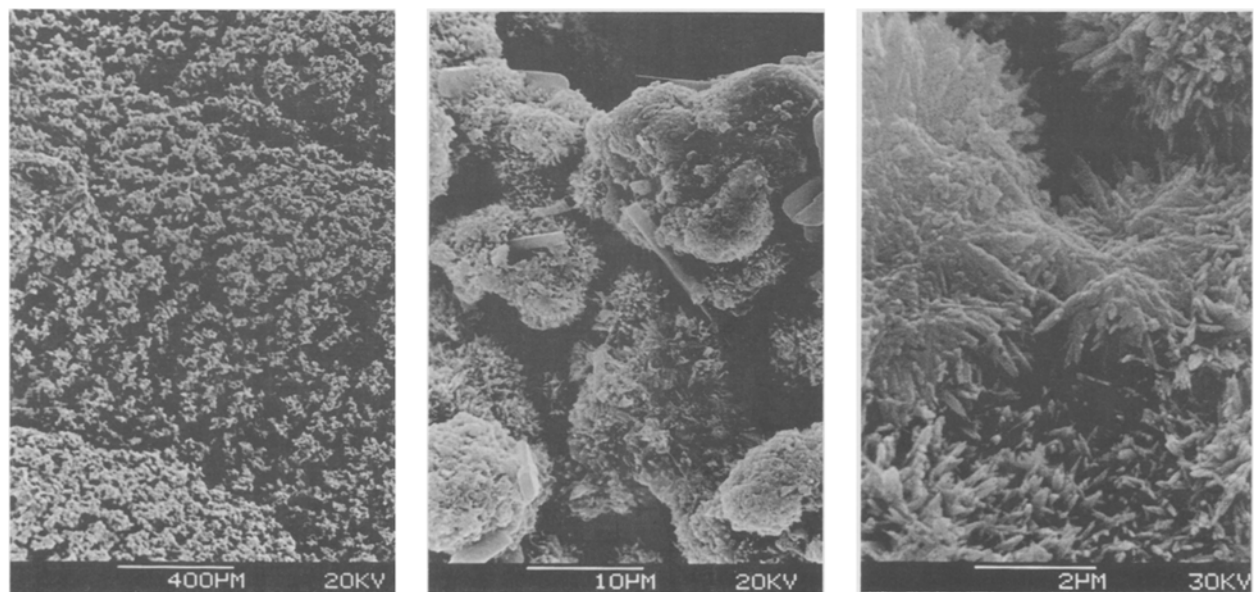


Fig. 7. Surface of EMD from a suspension bath, using hydrated $\text{MnO}_x \cdot y\text{H}_2\text{O}_1$ suspension (according to section 2c).

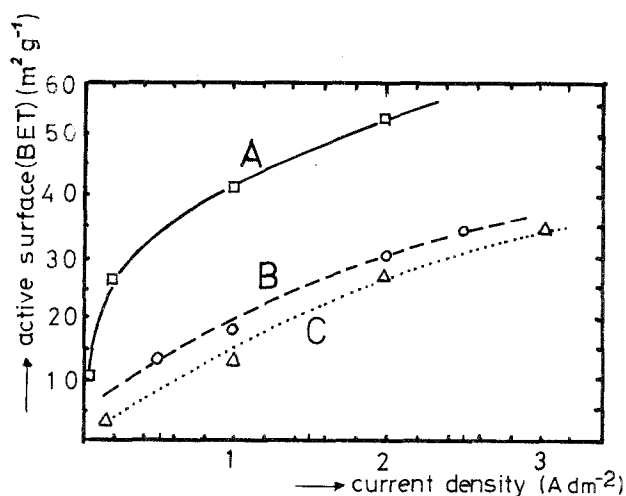


Fig. 8. Relation between the active surface, S_a , of 3 types of EMD and the current density of their deposition. (A) conventional bath ($\text{MnSO}_4/\text{H}_2\text{SO}_4$); (B) suspension bath ($\text{MnSO}_4/\text{H}_2\text{SO}_4$ + suspended EMD, $< 20 \mu\text{m}$); (C) fibrous EMD ($\text{Mn}(\text{ClO}_4)_2/\text{HClO}_4$, [6]).

In contrast to fibrous EMD no preferred crystal orientation can be observed in SBP-EMD deposits.

4. Discussion of the results

The experimental data given here can be explained by the model of EMD deposition presented previously [6]. This model describes how, at low current densities, $\gamma\text{-MnO}_2$ is deposited on the anode while at high current densities the less well crystallized $\varepsilon\text{-MnO}_2$ is formed. We now assume that in the suspension bath process the suspended particles are adsorbed on the surface of the anode and cause inhomogeneities in the local electrical field depending on their own electric conductivity. At these sites of adsorption new crystal nuclei of EMD originate.

The nuclei grow to form dendrites by which the real electrode surface is significantly enlarged.

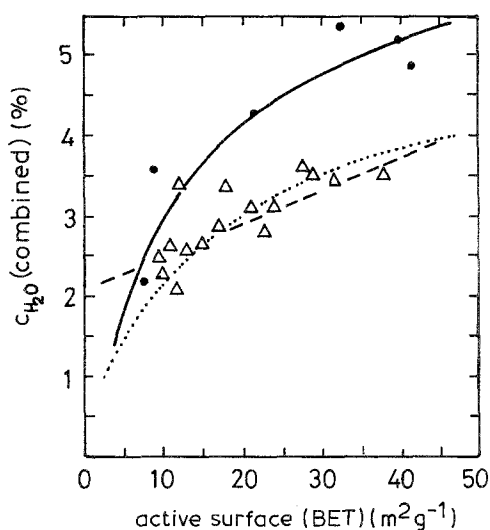


Fig. 9. Relation between the content of combined water ($c_{\text{H}_2\text{O}}$) and the active surface, S_a (BET), of fibrous EMD (\bullet) and SBP-EMD (Δ). Calculated curves: $c_{\text{H}_2\text{O}} = 3.47 \log S_a$ (FEMD) —; $c_{\text{H}_2\text{O}} = 2.09 \log S_a$ (SBP-EMD) \cdots ; $c_{\text{H}_2\text{O}} = 0.044 S_a$ (SBP-EMD) $---$.

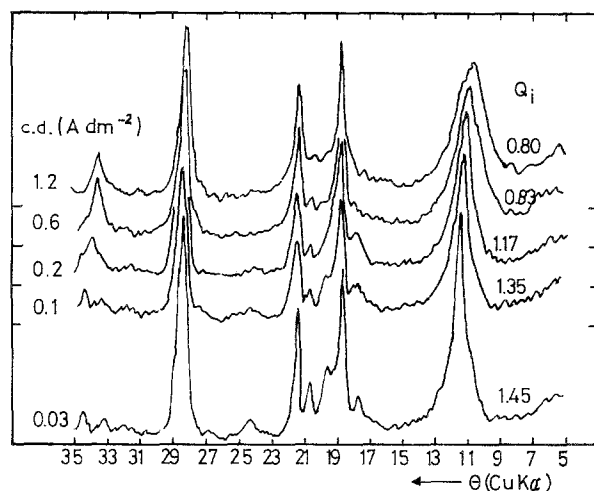


Fig. 10. X-ray diagrams of fibrous EMD from a manganese nitrate bath, deposited at 95°C and at different current densities (c.d.). Q_i is the intensity ratio of the reflections at $\theta = 11^\circ$ and $\theta = 18.5^\circ$.

On this enlarged effective surface the deposition proceeds with a low effective current density and, in consequence, the tendency to form $\gamma\text{-MnO}_2$ deposits increases.

The nuclei are adsorbed with random orientation, and so no texture of the dendrites can be observed. Therefore, the dendrites are not identical with FEMD fibers as has been suggested by Yoshio *et al.* [7, 9]. SBP-EMD cannot be readily cleaved as is the case with FEMD. Here, remarkable differences to FEMD are revealed.

Formation of $\gamma\text{-MnO}_2$ depends principally in the same manner on temperature and sulphuric acid concentration as does formation of $\varepsilon\text{-MnO}_2$ except that the latter is formed in the high current density region.

At higher particle concentrations higher adsorption rates are expected and consequently the decrease of

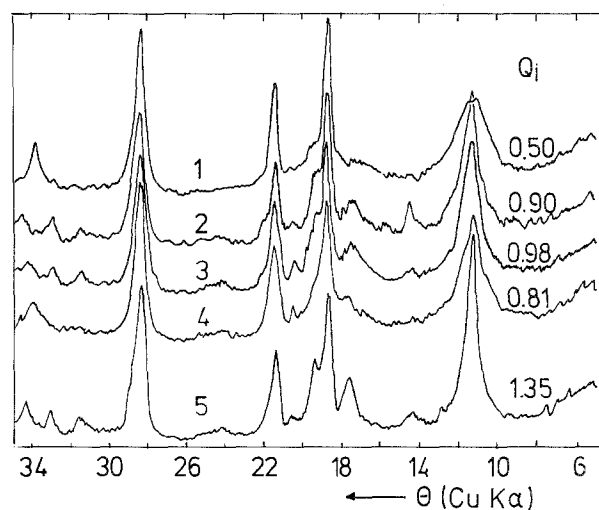


Fig. 11. Formation of EMD on the anode of a suspension bath as influenced by the addition of fine EMD powder. Sintered titanium anodes. (1) conventional bath ($i = 0.85 \text{ A dm}^{-2}$, $T = 95^\circ\text{C}$); (2) suspension bath (2 g/l EMD added, $i = 1.5 \text{ A dm}^{-2}$, $T = 95^\circ\text{C}$); (3) suspension bath (1 g/l EMD added, $i = 1.5 \text{ A dm}^{-2}$, $T = 95^\circ\text{C}$); (4) suspension bath (1 g/l EMD added, $i = 1.5 \text{ A dm}^{-2}$, $T = 90^\circ\text{C}$); (5) suspension bath (0.1 g/l hydrated MnO_x , $i = 0.85 \text{ A dm}^{-2}$, $T = 95^\circ\text{C}$).

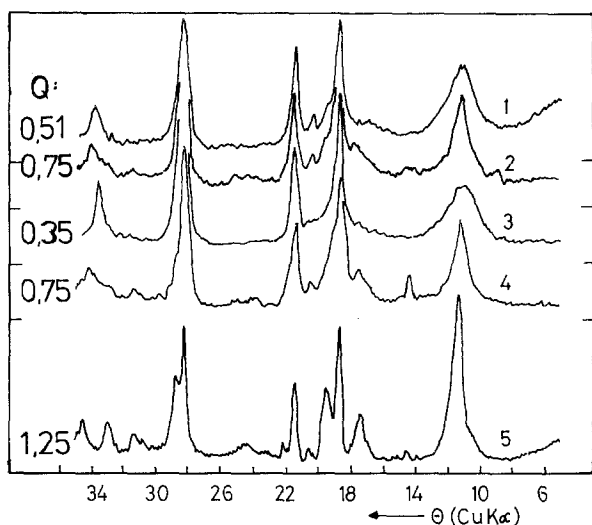


Fig. 12. Effectivity of particle type in a suspension bath to produce the shift from ϵ - to γ - MnO_2 structure at $T = 95^\circ\text{C}$ and c.d. 0.95 A dm^{-2} (1) conventional bath, no particle addition; (2) $0.20\text{ g/l Al}_2\text{O}_3$ fine particles (sulphate bath); (3) $0.20\text{ g/l Al}_2\text{O}_3$ fine particles (nitrate bath); (4) $2.0\text{ g/l } \beta\text{-MnO}_2$ fine particles; (5) $0.5\text{ g/l MnO}_x \cdot y\text{H}_2\text{O}$ (see reaction 2c).

the effective current density causes a higher proportion of γ - MnO_2 in the deposit. Therefore, continuous shift from ϵ - to γ - MnO_2 is possible.

Ultrafine nuclei such as $\text{MnO}_x \cdot n\text{H}_2\text{O}$ prepared by $\text{Mn}(\text{OH})_2$ oxidation, produce finer dendrites than do coarse nuclei (compare Figs 6b and 7).

It is quite possible that the adsorption of particles tends to saturation.

Completely non-conducting particles such as alumina do not cause the formation of SBP-EMD which seems to be in apparent contradiction with the result given in Fig. 12, pattern 2. Here the measure for γ - MnO_2 content, the ratio Q_i , was relatively high. The reason is that during a cycle of 14 days a certain amount of colloidal manganese dioxide precipitates from acid sulphate electrolytes and it is these particles, not the alumina, which produce the SBP effect. No such secondary effect arises from manganous nitrate baths (pattern 3 of Fig. 12) because no hydrous manganese oxide particles are precipitated.

The drop of the anode potential [7] on addition of Mn-oxide particles is easily explained by the reduction of the effective current density; reaction overvoltage is correspondingly reduced.

The ability of titanium anodes to resist passivation up to higher current densities in the suspension bath as compared to similar conditions in the conventional bath arises because γ - MnO_2 is a better electronic conductor than ϵ - MnO_2 (by a factor of about 10).

The electron concentration in the conduction band of γ - MnO_2 is larger by one order of magnitude compared with that of ϵ - MnO_2 . Therefore, a higher tunneling current density can be sustained at the phase boundary Ti-TiO_2 - γ - MnO_2 than at the phase boundary Ti-TiO_2 - ϵ - MnO_2 [14] until electron depletion results in ionic current transport and, consequently, growth of the TiO_2 interlayer.

The mechanical properties of the SBP-EMD differ remarkably from the glass like conventional EMD. In the latter, large internal stresses often arise within the deposit. These cause irregular fractures in unpredictable directions and as a result descaling is a common feature with large and planar anodes. High-grade SBP-EMD deposits do not exhibit similar behaviour. Obviously the intergrowth of dendrites in several directions and the voids between the dendrites reduce the internal stresses and avoid the propagation of crevices.

No explanation can be given for the influence of nitrogen or argon gas on the deposits of the suspension bath which was described by Yoshio *et al.* [7] and by Holzleitner *et al.* [9]. No effects due to stirring or to nitrogen gas introduction into the electrolysis cell were found in this work. Further experimental investigations are needed to understand this difference.

References

- [1] J. M. Fisher and A. Carter, in 'The 2nd Battery Materials Symposium (Eds. K. Kordesch and A. Kozawa) Vol. 2, Graz, (1985) IBA Cleveland, Paper No. 24 (1986).
- [2] E. Preisler, *Chem.-Ing.-Tech.* **49** (1977) 347.
- [3] E. Preisler and G. Mietens, *Dechema Monogr.* Vol. 109, Verlag Chemie, Weinheim (1987) 123-37.
- [4] M. Misawa, K. Matsuura and T. Okuda, *Jap. Pat.* 57-1087 (1982).
- [5] M. Misawa, T. Okuda and K. Matsuura, *Jap. Pat.* 57-42711 (1982).
- [6] E. Preisler, in 'The 2nd Battery Material Symposium', (Eds. K. Kordesch and A. Kozawa) Vol. 2, Graz, (1985) IBA, Cleveland, Paper No. 17 (1986).
- [7] M. Yoshio and H. Noguchi in 'The 2nd Battery Materials Symposium, (Eds. K. Kordesch and A. Kozawa), Vol. 2, Graz (1985) IBA, Cleveland, Paper No. 18, (1986).
- [8] G. W. Mellors, (to Union Carbide Corp.), US 4,549,943 (Appl. Nov. 11, 1984).
- [9] K. Holzleitner, M. Yoshio, H. Noguchi, H. Kurimoto and N. Miyamoto, submitted for publication in 'Progress in Batteries and Solar Cells', Vol. 7, 1988.
- [10] E. Preisler, G. Nolte, J. Holzem and G. Sorbe (to Hoechst AG) DE-OS 37 03 616 (06.02.1987).
- [11] E. Preisler in 'The 2nd Manganese Dioxide Symposium', (Eds. B. Schumm, H. M. Joseph and A. Kozawa) Tokyo (1980) I.C. Sample Office Cleveland, Ohio, USA, (1981) p. 184.
- [12] P. M. de Wolff, I. W. Visser, R. Giovanoli and R. Brüttsch, *Chimia* **32** (1978) 257-59.
- [13] P. M. de Wolff, *Acta Cryst.* **12** (1959) 341.
- [14] E. Preisler, accepted for publication in *J. Appl. Electrochem.*
- [15] P. Ruetschi, *J. Electrochem. Soc.* **131** (1984) 2737.